JOURNAL OF THERMOPHYSICS AND HEAT TRANSFER
Vol. 7, No. 3, July–Sept. 1993

Electrode Phenomena in High-Current, High-Pressure Arc Heaters

P. Durgapal*
Eloret Institute, Moffett Field, California 94035

The behavior of an arc in the cathode region of a high-pressure, high-current arc heater is investigated numerically. The study is conducted to determine the design features required for high-performance arc heaters needed for future aerospace research facilities. Computations are performed for operating pressures in the range 50–200 atm and load currents in the range 6000–18,000 amp. At high pressures, due to the high-current carrying capability of the dense gas, spot size remains reasonably small, even for high-load currents. Its value is 1.1 mm for a 50-atm arc with a load current of 18,000 amp. By increasing pressure, it can be reduced further. Smaller spot size may allow us to design thinner electrode rings. Spot temperatures are high enough to cause ablation of the electrode material. In order to reduce material ablation at very high currents and prolong electrode life, the operating pressure must be high and the arc should be rotated. Experimental studies to compare with these results would be desirable.

Nomenclature

A_{rate} = rate of material loss, g/s
A_{rich} = Richardson's constant, A/m^2/K^2
$\boldsymbol{B}$ = magnetic field strength, T
C_D = drag coefficient
c = specific heat, J/kg
$\boldsymbol{E}$ = electric field vector, V/m
e = electronic charge, C
F = heat of ablation, J/kg
I = load current, amp
$\boldsymbol{J}$ = current density vector, amp/m^2
j = current density, amp/m^2
K = thermal conductivity, W/m/K
k = Boltzmann constant, J/K
L = length of arc foot, m
m_i = mass of ions, kg
N = number density, m^3
n_e = electron number density, m^3
P = pressure, atm
R = inner radius of the electrode, m
R_s = radius of the spot, m
r = radial coordinate
s = electrode pitch, m
T = temperature, K
u = local gas velocity, m/s
V_a = ablation velocity, m/s
V_c = sheath voltage, V
v = average gas velocity, m/s
v_a = velocity of the arc foot, m/s
z = axial coordinate
ε_w = reflectivity of the wall
μ_0 = permeability of free space, H/m
ρ = density, kg/m^3
σ = electric conductivity, mho/m
$\phi_i(\phi_I)$ = ionization (excitation) potential, eV
ϕ_w = work function, eV
ψ = stream function

Presented as Paper 92-0810 at the AIAA 30th Aerospace Sciences Meeting and Exhibit, Reno, NV, Jan. 6–9, 1992; received March 16, 1992; revision received Aug. 3, 1992; accepted for publication Aug. 14, 1992.

*Research Scientist, M/S 229-4, NASA Ames Research Center. Member AIAA.

I. Introduction

IN recent years there has been increased interest in planetary missions. Such missions will involve atmospheric entries at velocities substantially greater than those experienced by the space shuttle. High-enthalpy and high-pressure arc jets are needed to simulate re-entry from interplanetary missions and to provide test media for hypersonic research. Also, there has been some interest in using high-enthalpy arc jets as front-end add-ons to a high-enthalpy flowing facility for aerodynamic studies. In order to achieve hypersonic velocities, the arc jets must be operated at high pressures, and to achieve the required enthalpies at those high pressures we must increase the load current. The development of such highly energetic advanced capability requires improved arc-jet technology and a better understanding of the physics of arcs encountered in different regions of the arc heater. In order to achieve the goal of high enthalpy and high pressure at the same time, we will have to draw high-load current in a high-pressure environment. Under these conditions, one of the main problems is the failure of the electrodes.

The purpose of this article is to study the characteristics of a high-pressure, high-current arc in the downstream electrode region (cathode) of an arcjet. For this, a model developed in a previous paper[1] is used. In the first part, a summary of this model is presented. This includes the following:

1) A description of the axisymmetric model used to generate profiles of the electrical characteristics in the downstream electrode region (cathode) of an arc jet is given. The gas-dynamic motion of the gas flowing through the heater is not included in this model. For computations of thermodynamic properties of the gas, a separate one-dimensional model of arc heating based on radiative and convective heat transfer (described in Ref. 1) is used.

2) A model for arc termination at the electrode wall is given. The model relates the ion and electron currents to the spot size and temperature using several energy balance equations.

In the second section, results are presented. Current density distribution for a cathode region with multiple electrodes for a high-pressure, high-current arc is discussed. Computations for stationary arcs are not presented, because at high pressures and high currents the ablation velocity is very large and this causes deep erosion of the electrodes. Thus, for high-current and high-pressure operation, it is absolutely necessary to rotate the arc so that the ablation of the electrode material remains under control. For this reason, all results will be shown for rotating arcs only.

Results are computed for copper and tungsten, as these two materials are most commonly used in the construction of electrodes.

II. Physical Model

The theoretical model of the electrode phenomena in arc jets has been described in detail in Ref. 1. In reality, this is a three-dimensional problem, but for simplicity it is modeled in two steps. In the first step, an axisymmetric current distribution is determined, assuming that current terminating at the electrode segment is uniformly distributed around the electrode perimeter. The analysis provides the axial and radial distribution of the current density. The second step in the model is the analysis of the arcfoot, a termination point of the central arc column of a given electrode. Now it is assumed that the disk of uniform current distribution transforms into a spoke and terminates at a certain location on the electrode.

For referencing, results of the relevant equations need to be described here. These consist of the following:

A. Current Distribution

An axisymmetric model[1] describing the electrical characteristics in the downstream electrode region (cathode) of an arc jet are discussed. The basic equations used are Maxwell's equations and the generalized Ohm's law. To evaluate the current density distribution, the conventional stream function concept is used. ψ is defined as

$$\left.\begin{aligned} J_z &= \frac{1}{r}\frac{\partial}{\partial r}(r\psi) \\ J_r &= -\frac{\partial \psi}{\partial z} \end{aligned}\right\} \tag{1}$$

where J_z and J_r are the axial and radial components of the current density. Equation (1), together with Ohm's law, leads to the following second-order differential equation for the stream function:

$$\frac{\partial}{\partial r}\left[\frac{1}{r}\frac{\partial(r\psi)}{\partial r}\right] + \frac{\partial^2\psi}{\partial z^2} - \frac{1}{\sigma}\frac{\partial \sigma}{\partial r}\left(\frac{\psi}{r} + \frac{\partial \psi}{\partial r}\right) - \mu_0 \sigma v \frac{\partial \psi}{\partial z}$$

$$- \frac{1}{\sigma}\frac{\partial \sigma}{\partial z}\frac{\partial \psi}{\partial z} + \frac{\sigma}{en_e^2}\frac{\partial n_e}{\partial r}\frac{\partial p_e}{\partial z} - \frac{\sigma}{en_e^2}\frac{\partial n_e}{\partial z}\frac{\partial p_e}{\partial r} = 0 \tag{2}$$

Equation (2), together with necessary boundary and subsidiary conditions typical of the electrode region, is then solved using Gauss-Seidel successive relaxation technique. Profiles for the stream function and the current density are obtained as a result of this analysis.

B. Arc Foot Parameters

The next step is the analysis of the arc foot. For this study a single electrode is considered. The current density distribution at different locations on the electrode is determined using the electromagnetic code described above. Electric field is determined at the location where current concentration is maximum. This is the location where the arc foot will terminate at the wall. In the model presented here, ions are accelerated through a sheath to the cathode by the cathode voltage drop. Both kinetic and ionization energies are transferred to the cathode. A spot forms at the location where this transfer of energy occurs. The size and temperature of this spot are estimated from an energy balance between the heat transferred to the cathode by the ions and the heat transferred from the spot by conduction in the cathode. The ions are created by electron collisions in the air in a region near the cathode. The electrons are thermionically emitted from the cathode. The same cathode voltage drop which accelerates the ions to the cathode, also accelerates the thermionically emitted electrons from the cathode into this ionization region.

If there is no mass transfer from the cathode then, the steady-state energy balance is given by[1,2]

$$4R_sK(T_s - T_w) = \pi R_s^2[j_i(V_c + \phi_i - \phi_w)$$

$$+ j_I\phi_I - j_e\phi_w - \varepsilon_w\sigma(T_s^4 - T_w^4)] \tag{3}$$

where T_s is temperature of the spot, T_w is wall temperature away from the spot, j_e is the electron current, j_i is the ion current, and σ is the Stefan-Boltzmann constant. The left side of this equation gives the energy conducted from the spot to the surrounding material. The first two terms on the right give the energy transported by the ion flux, the third term gives the energy carried by the electron current emitted from the spot, and the last term gives the net heat transfer by radiation. The electron current is related to the spot temperature by the Richardson equation[3]

$$j_e = A_{\text{rich}}T_s^2 \exp[-(e\phi_w/kT_s)]\cdot\exp(4.389\sqrt{E}/T_s) \tag{4}$$

where E is in V/cm.

The ratio of ion and electron currents is obtained by an energy balance in the ionization region

$$\frac{j_i}{j_e} \equiv \gamma_i = \frac{V_c - \frac{1}{2}(\phi_i - \phi_I)}{\phi_i + \frac{1}{2}(\phi_i - \phi_I)} \tag{5}$$

From the expression for the total current, one can obtain the radius of the spot

$$R_s = \sqrt{[I/\pi(j_e + j_i)]} \tag{6}$$

The ion current is given by random thermal current

$$j_i = \tfrac{1}{4}eN_iv_i$$

where

$$v_i = \sqrt{(8kT_i/\pi m_i)}$$

If the pressure in the ionization region is assumed to be the same as in the rest of the gas, then

$$(P/kT) = N = N_0 + N_I + N_i + (T_e/T)N_e \tag{7}$$

If the electron temperature T_e is much larger than the ionization temperature, and the degree of ionization is greater than 30%, the sum $(N_0 + N_I)$ of neutral and excited state number densities can be neglected in Eq. (7) to give

$$N = N_i + (T_e/T)N_e$$

It is assumed that the gas consists of singly ionized atoms only $(N_i = N_e)$. This yields

$$N_i = [1/(1 + \theta)]N$$

where $\theta = T_e/T$ and N is the total density. The ion temperature T_i is assumed to be equal to the neutral temperature, and both are assumed to be the same in the ionization and discharge region. In order to determine the electron temperature in the ionization region, it is assumed that the average energy of the electrons is less than the energy required for ionization from the first excited state, since this is the elastic collision with the smallest energy transfer from the electron to the atom, and hence, the smallest mean free path. It may be assumed that the distribution of electrons with energy less than this energy will be such that the average energy will be one-half of this energy, i.e.

$$\tfrac{3}{2}kT_e = \tfrac{1}{2}e(\phi_i - \phi_I) \tag{8}$$

Thus, the ratio of temperatures becomes

$$\theta = \frac{T_e}{T_i} = \frac{e(\phi_i - \phi_f)}{3kT_i} \tag{9}$$

The nonlinear Eqs. (3) and (5) are solved simultaneously to yield the spot temperature and the sheath voltage. The radius of the spot is calculated from Eq. (6).

When the spot temperature is greater than the melting point of the electrode material, then the total rate of material lost is calculated using a heat balance at the spot, and is given by

$$A_{\text{rate}} = V_a \pi R_s^2 \rho_m \tag{10}$$

where the ablation velocity[4] is given by

$$V_a = \frac{(q/A)_0}{\rho_m F\{1 + [c(T_s - T_w)/F]\}} \tag{11}$$

where $(q/A)_0$ is the heat flux to the arc spot, ρ_m is the electrode material density, and T_w is the electrode wall temperature.

In order to minimize the erosion of the electrode due to the current concentration, an axial magnetic field is applied to the arc foot by a magnet coil built inside each electrode segment. The arc foot rotates in a radial plane under the influence of the Lorentz force. A steady state is reached when the magnetic force is balanced by the aerodynamic drag on the arc. In analogy, with the drag coefficient on a solid cylinder in a flow, a drag coefficient can be defined as[5,6]

$$C_D = \frac{IBL}{\frac{1}{2}\rho_\infty v_a^2 (2R_s L)} \tag{12}$$

where ρ_∞ is the density of the surrounding gas. L is same as the radius of the electrode in our case. The rotation velocity of the arc foot is determined from Eq. (12). Experiments show that C_D can be approximated by using the drag coefficient of a rotating hot solid cylinder under similar fluid mechanical conditions. The variation of the drag coefficient with the Reynold's number is taken from the experimental data.[1,5,6] Reynold's number R_e is based on the freestream velocity, density, diameter of the arc foot, and the kinematic viscosity evaluated at the boundary of the arc and the surrounding gas.

III. Results

In the results presented here, it is assumed that the cathode region consists of four electrodes, each with a radius of 5.2 cm and a width of 2 cm. Electrodes are separated from each other by an insulator ring with a width of 1.2 cm and a radius of 5.2 cm. Thermal properties are generated using a simple heat transfer model discussed in Ref. 1. This model assumes that heat is added to the fluid by Joule heating in the central arc core region. Due to its high temperature, this region transfers some of its energy to the surrounding cooler gases by way of convective and radiative heat transfer. Table 1 presents the operating conditions for which the results are computed. It is anticipated that future arc heaters will be able to function under these conditions.

Table 1 Operating conditions

Number	Load current, kA	Pressure, atm	Mass flow, kg/s	Input power, MW
1	6	50	3	77.07
2	10	50	3	131.07
3	14	50	3	173.58
4	18	50	3	199.57
5	10	100	6	189.82
6	10	150	3	238.50
7	10	200	3	257.81

Figure 1 displays a plot of the current density distribution for a load current of 6000 A at 50 atm. The basic appearance of this plot is similar to that for 1 atm (Ref. 1). However, the magnitude of the current density on the electrode surface is different. Initially, the current is concentrated near the axis, which is the core of the arc. Due to the subsidiary condition that current be equally shared by all the electrodes, at each electrode surface $\frac{1}{4}$ of the current terminates. Beyond the fourth electrode, the current density distribution becomes insignificant. The current density on the surface, of say, the first electrode of the four electrode configuration, is about four times less than that for a single electrode configuration.

For simplicity, the arc foot parameters are investigated for a single electrode. For all cases, arc foot parameters are computed at the second electrode of the four-electrode assembly. Electric field is calculated at the point where the current density is maximum on this electrode. The arc foot is assumed to terminate at the point where the electric field is maximum.

Computations are carried out for load currents in the range 6000–18,000 A, and pressures in the range 50–200 atm. Each figure is shown for two electrode materials, namely copper and tungsten. In the results shown, all computations are done for rotating arcs only. The reason for this is that at the high values of pressure and current considered, spot temperatures exceed the melting point of the electrode material. Furthermore, if the arc is kept stationary, the rate of material loss is very high. For instance, for an 150-atm arc and load current of 10,000 A, the ablation rate for copper is 0.5 g/s, while for tungsten it is 1.28 g/s. Such high rates of material loss will lead to deep erosion of the electrodes, and finally its destruction in seconds.

The arc foot is rotated by applying an axial magnetic field which is produced by a magnetic coil built inside each electrode segment. In the present computations, a $4\frac{1}{2}$-turn built-in coil is assumed. The magnetic field is proportional to the arc current and achieves values of the order of 2000 G for the range of currents considered.

Figures 2–5 illustrate the spot parameters as a function of load current at constant pressure. It is observed that all the parameters increase with the increase in load current. Figure 2 shows that the spot size increases with load current, but it is still very small. It is about 1.1 mm for a current of 18,000 A for both copper and tungsten. In comparison, for an atmospheric arc,[1] the spot radius, for a load current of 3000 A, was found to be considerably larger, about 3.2 mm. The spot temperatures (Fig. 3) for copper are slightly higher than those for tungsten. For a load current of 18,000 A, their values are about 4975 and 4925 K, respectively.

Figure 4 shows the ablation rate as a function of load current for $P = 50$ atm. For copper, the ablation rate increases from 1.92 to 5.32 mg/s as load current increases from 6000 to 18,000 A. For the same range of current, ablation rate for tungsten increases from 5.36 to 14.8 mg/s. Therefore, copper seems to be a better candidate for electrode material, even at high values of load currents. The flow enthalpy as a function of load current is also plotted in Fig. 4. Thus, a given achievable flow enthalpy can be related with an ablation rate associated with it, for $P = 50$ atm.

Figure 5 shows that at constant pressures, arc foot rotation frequency is almost a linear function of load current and is independent of the material of the electrode.

Figures 6–10 illustrate the behavior of arc foot parameters as a function of pressure. It is observed that the temperature of the spot and ablation velocity increase with pressure while the radius of the spot, ablation rate, and arc rotation frequency decrease. The spot radius, for $I = 10{,}000$ A, decreases by 50% as pressure increases from 50 to 200 atm.

Figures 8 and 9 show that ablation rate and ablation velocity for tungsten are much larger than those for copper. At 50 atm, the ablation rate for tungsten is about 2.8 times that for copper, while at 200 atm, this factor reduces to 2.59. The ablation rate for copper decreases 3.5 times as pressure is

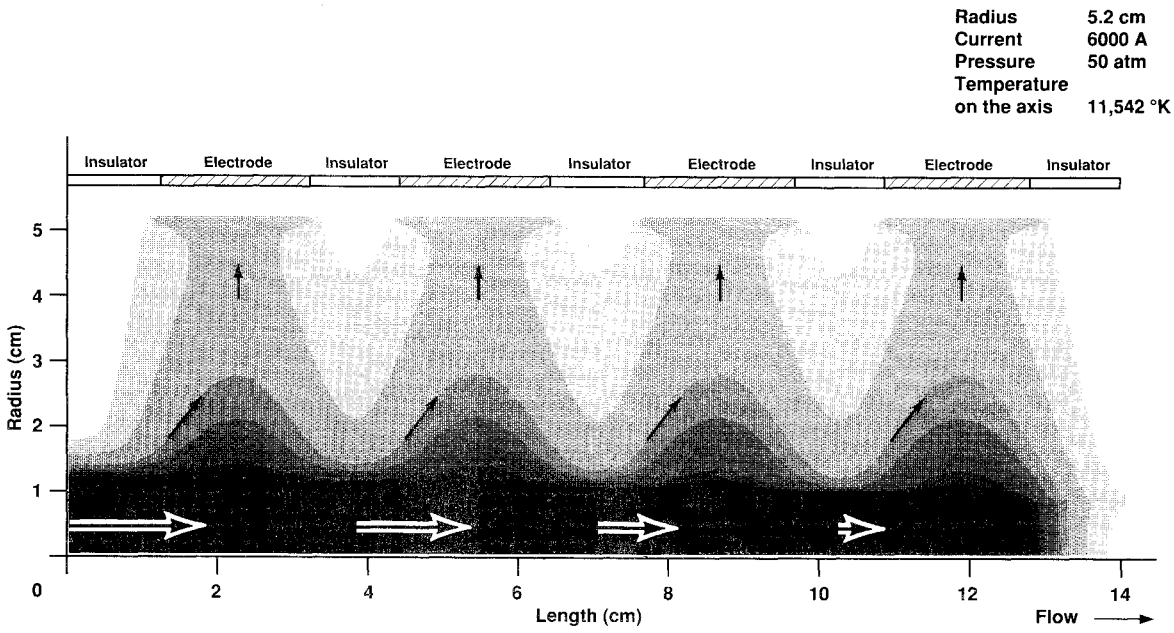

Fig. 1 Current density distribution for a four-electrode assembly at high pressure. P = 50 atm, I = 6000 A, T_w = 1000 K, $\dot{m}$ = 3.0 kg/s.

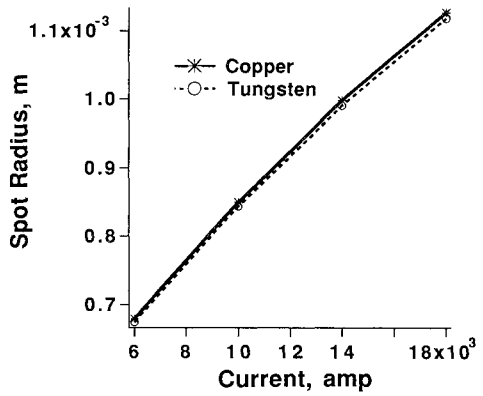

Fig. 2 Variation of spot radius with load current. Pressure = 50 atm.

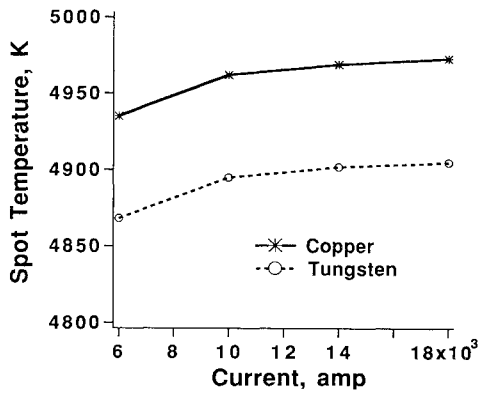

Fig. 3 Variation of spot temperature with load current. Pressure = 50 atm.

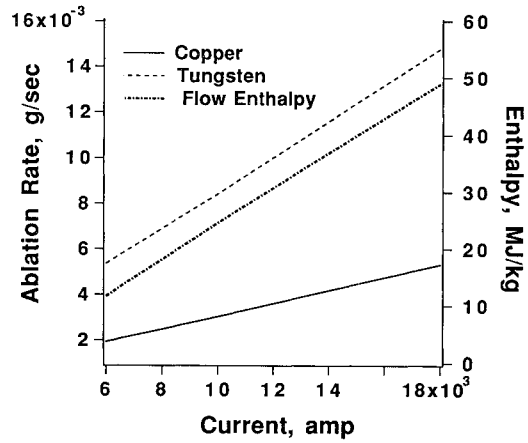

Fig. 4 Ablation rate and flow enthalpy as a function of load current. Pressure = 50 atm.

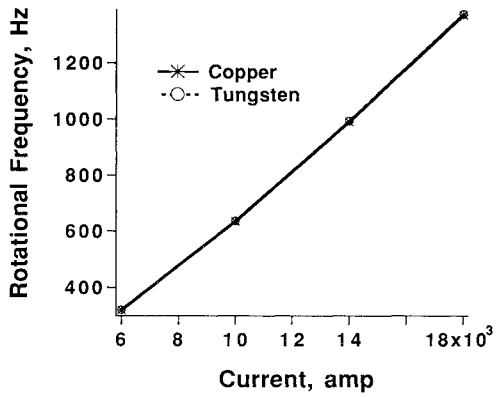

Fig. 5 Rotation frequency of the atmospheric arc as a function of load current. Pressure = 50 atm.

increased from 50 to 200 atm for a load current of 10,000 A. For the same conditions, the decrease in the ablation rate of tungsten is 3.8 times.

Increase in pressure also leads to reduced arc rotation frequency. Figure 10 shows that rotation frequency decreases by more than 30% when pressure is increased from 50 to 200 atm.

IV. Discussion

The main problem associated with high-current, high-pressure arcs, is that the spot temperature is very high. Rotation of the arc is a must under these conditions, since large ablation velocity for a stationary arc results in deep erosion of the electrode. Copper seems to be a good candidate for electrode material, even for high-current, high-pressure arcs, since the total rate of material loss for copper is less than that for tungsten under identical conditions. When working with high-load currents, maintaining high pressure is a necessity since

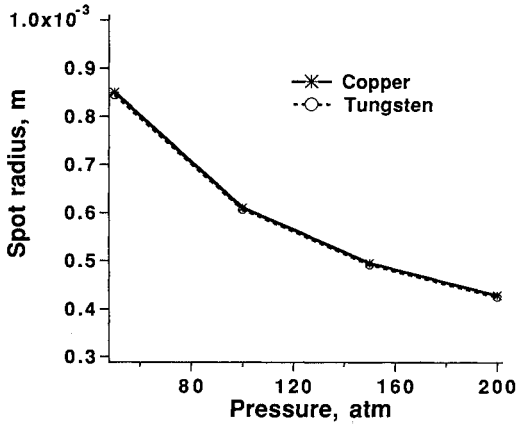

Fig. 6 Variation of spot radius with pressure. I = 10,000 A.

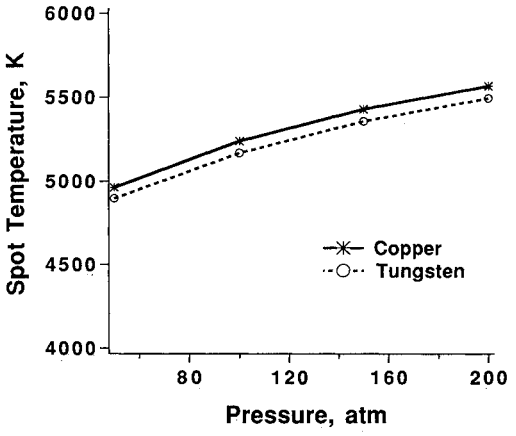

Fig. 7 Variation of spot temperature with pressure. I = 10,000 A.

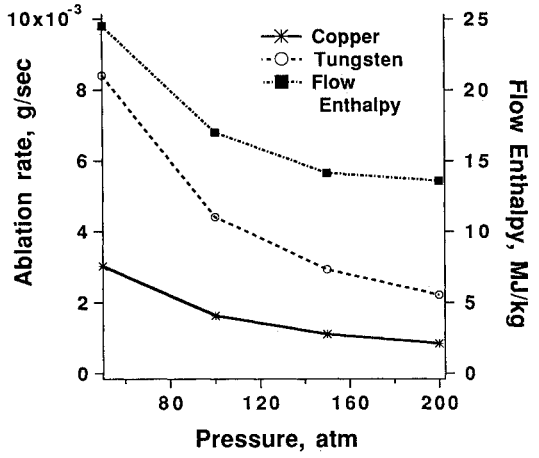

Fig. 8 Ablation rate and flow enthalpy as a function of pressure. I = 10,000 A.

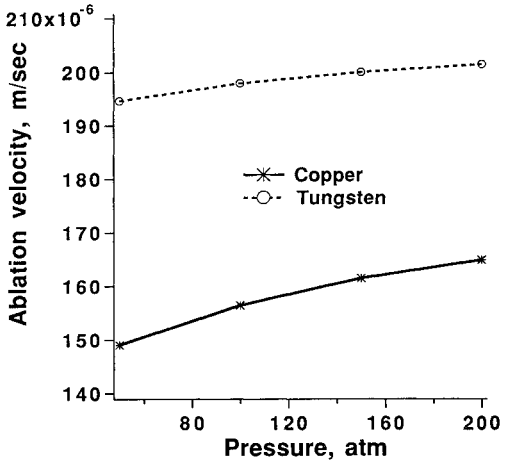

Fig. 9 Ablation velocity on the surface of copper electrode as a function of pressure. I = 10,000 A.

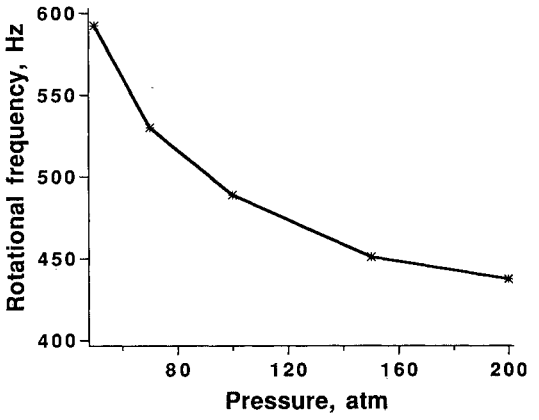

Fig. 10 Rotation frequency of the atmospheric arc as a function of pressure. I = 10,000 A.

higher pressures lead to reduction in ablation rate and spot radius. If the levels of ablation rates allowed for a reasonable operational electrode life were known, then it would be possible to predict the achievable flow enthalpy for any given operational pressure. But, at present, no quantitative data on ablation rates are available.

Note that enthalpy also decreases as pressure increases. In order to maintain the same level of enthalpy, the load current will have to be increased. Since spot size also decreases as pressure increases, it may be possible to use thinner electrodes. Increased load current will result in higher current concentration on the electrodes. In order to reduce this increased current concentration, the number of electrode rings in the electrode assembly can be increased. Thus, by having thinner electrodes, the number of electrode rings can be increased without making the electrode assembly very cumbersome. The observation that the ablation velocity increases with pressure and the spot radius decreases with pressure, is indicative of the fact that the rate of loss of electrode material will be large, but the craters created will be small in size. The reason for this could be that as pressure and gas density increase, for the same electron mole fraction, the electron number density increases. For the same load current this will result in higher values of j_e, which in turn will lead to smaller spot size [see Eq. (6)]. For the same ablation rate, if the spot size is small, the ablation velocity will be large.

At the present time, experimental data for arc foot parameters are not available, even for atmospheric arcs at lower load currents. Availability of such data is highly desirable so that some confidence can be put in the numbers obtained by the present analysis.

V. Conclusions

In the first part of this article an analysis of the electrical characteristics is conducted. It is observed that the basic appearance of the current density distribution resembles that for the atmospheric arc at lower currents,[1] but the magnitude of the current density on the surface of the electrode is different. In the second part, spot parameters are computed. Spot size is reasonably small even for very large currents. Its value is about 1.1 mm for a 50-atm arc with a load current of 18,000 A. When pressure is increased from 50 to 200 atm, the spot size decreases by 50%. Due to smaller spot radii at high pressures, it may be possible to design thinner electrodes, and in this way facilitate the increase in the number of electrodes for high-current operation without making the assem-

bly too large. In order to reduce electrode erosion, rotation of the arc is necessary.

Given an allowed ablation rate of the electrode material for a given electrode life, the maximum achievable flow enthalpy in the arc jets can be estimated. Copper is a better electrode material for high-current and high-pressure operations.

Acknowledgment

This work was supported by NASA Grant NCC-2-688.

References

[1]Durgapal, P., "Current Distribution in the Cathode Area of an Arc Heater," *Journal of Thermophysics and Heat Transfer* (to be published); see also AIAA Paper 91-1385, June 1991.

[2]Nichols, L. D., and Mantenieks, M. A., "Analytical and Experimental Studies of MHD Generator Cathods Emitting in a 'Spot' Mode," NASA TN D-5414, Sept. 1969.

[3]Cobine, J. D.,"Emission of Electrons and Ions by Solids," *Gaseous Conductors*, 1st ed., Dover, New York, 1958, pp. 106–122.

[4]Rohsenov, W. M., and Choi, H., "Heat Transfer in Stationary Systems," *Heat, Mass and Momentum Transfer*, Prentice-Hall, Englewood Cliffs, NJ, 1961, p. 122.

[5]Winograd, Y. Y., and Klein, J. F., "Electric Arc Stabilization in Crossed Convective and Magnetic Fields," *AIAA Journal*, Vol. 7, No. 9, 1969, pp. 1699–1703.

[6]Roman, W. C., and Myers, T. W., "Experimental Investigation of an Electric Arc in Transverse Aerodynamic and Magnetic Fields," *AIAA Journal*, Vol. 5, No. 11, 1967, pp. 2011–2017.